

Dynamic proton model for the hyperfine structure of the hydrogenlike ion ${}^{209}_{83}\text{Bi}^{82+}$

L.N. Labzowsky

Department of Physics, St. Petersburg State University, Petrodvorets, St. Petersburg, Russia

W.R. Johnson* and G. Soff

Institut für Theoretische Physik, Technische Universität Dresden, D-01062 Dresden, Germany

S.M. Schneider

Institut für Theoretische Physik, Johann Wolfgang Goethe-Universität, D-60054 Frankfurt am Main, Germany

(Received 9 December 1994)

The hyperfine structure of the one-electron ion ${}^{209}_{83}\text{Bi}^{82+}$ is evaluated within the framework of a dynamical model in which the electron is assumed to interact with the valence proton through the exchange of a photon.

PACS number(s): 31.30.Gs, 31.30.Jv, 31.15.Ar

I. INTRODUCTION

Measurements of the hyperfine structure (hfs) of highly charged one-electron ions can provide tests of QED in strong fields. To this end, a precise measurement of $F = 5$ to $F = 4$ hyperfine interval in the ground state of ${}^{209}_{83}\text{Bi}^{82+}$ has been carried out recently [1]. This measurement can be compared with recent calculations of the ${}^{209}_{83}\text{Bi}^{82+}$ hfs based on the external-field approximation that have been carried out within the framework of QED [2-6]. In these calculations, two principal corrections to the basic Fermi-Breit formula were taken into account: the magnetic moment distribution within the nucleus [2,3,6] and radiative corrections [4,5]. Both of these corrections are of comparable size.

Here we develop a dynamic model for the hfs of ${}^{209}_{83}\text{Bi}^{82+}$ that takes into account explicitly the proton motion inside the nucleus and, therefore, includes the effects of a distributed nuclear magnetic moment automatically. The model treats the motion of the proton and of the electron relativistically. In the point-nucleus limit, the model reduces to the usual static model, but with a relativistic independent-particle value for the nuclear moment. The relativistic moment is found to be about 3% smaller than the observed moment of ${}^{209}_{83}\text{Bi}$. In the nonrelativistic proton limit, the correction for the finite distribution of magnetization obtained from the model, the Bohr-Weisskopf (BW) correction, reduces to that obtained previously in the nonrelativistic single-particle approximation [7-9].

The dynamical model allows for calculations of radiative corrections using the standard rules of QED. It can also be generalized to permit a many-body description of the nucleus, including the core polarization corrections and the collective effects which are responsible for the

deviation of the observed magnetic moment of ${}^{209}_{83}\text{Bi}$ from the single-particle limit.

In our applications, we ignore both radiative corrections and nuclear many-body corrections. To compare with experiment and with earlier calculations, we replace the magnetic moment given by the model with the measured magnetic moment. In the point-nucleus approximation, the present calculations then coincide with those from Ref. [3]. The value of the BW correction depends on the details of the nuclear potential. We assume that the nuclear potential is a Woods-Saxon potential with parameters chosen to reproduce the experimental proton binding energy and to give a magnetization distribution function with the same root-mean-square radius as the distribution function used in [3]. With that choice, the finite nuclear magnetization correction found here differs with that found in Ref. [3] by about 10%. The principal reason for this difference is that the expression for the BW correction used in [3] assumes that the nuclear spin distribution is spherically symmetric, while the present model predicts an asymmetric spin distribution.

II. MODEL

We treat the valence proton and the electron in ${}^{209}_{83}\text{Bi}^{82+}$ as a system of two interacting particles. Both particles move in the field of the nucleus and interact with one another by exchange of photons. We use the Furry picture in QED and describe the proton as a Dirac particle moving in a central potential $U(r)$ determined by the strong interactions. The electron is also described as a Dirac particle, but moving in the Coulomb potential $V^{(Z-1)}(r) = -(Z-1)n(r)/r$, corrected by the function $n(r)$ for the finite nuclear charge distribution. We do not include the proton's anomalous moment in our model since our aim is to describe the interaction of the electron with a proton in a high orbital angular momentum state, $L = 5$, where the nuclear gyromagnetic ratio is

*Permanent address: Department of Physics, Notre Dame University, Notre Dame, IN 46556.

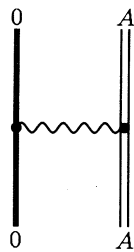


FIG. 1. Feynman graph describing the Breit interaction between proton in state $|0\rangle$ and electron in state $|A\rangle$. The thick line designates the proton, the double line designates the electron in the field of the core, and the wavy line designates the transverse photon.

dominated by orbital contributions.

The principal contribution to hfs is given by the Feynman graph of Fig. 1, describing the Breit interaction between two particles. This contribution can be evaluated in the Furry picture to give

$$\Delta E_{\text{hfs}} = \langle V_{\text{Br}} \rangle_{0A,0A} = \left\langle \frac{\boldsymbol{\alpha}_p \cdot \boldsymbol{\alpha}_e}{r_{12}} \right\rangle_{0A,0A}. \quad (1)$$

Here $\boldsymbol{\alpha}_p$ and $\boldsymbol{\alpha}_e$ are Dirac matrices for the proton and electron, respectively, and $r_{12} = |\mathbf{r}_p - \mathbf{r}_e|$. We consider the proton as a particle with a normal Dirac magnetic moment. The two-particle wave functions $|0A\rangle$ are product wave functions coupled to a fixed value of total angular momentum. In Eq. (1), and throughout the remainder of the paper, we use atomic units.

Consider now the second-order graph in Fig. 2. This graph gives the Coulomb correction to the hfs:

$$\Delta E_{\text{hfs}}^{(1)} = \sum_{Nn} \frac{\langle 0A | V_{\text{Br}} | Nn \rangle \langle Nn | V_{\text{C}} | 0A \rangle}{E_0 - E_N + \epsilon_A - \epsilon_n}. \quad (2)$$

Here $V_{\text{C}}(r) = -1/r$ is the Coulomb interaction between the proton and electron. The proton and electron energies are denoted by E_N and ϵ_n . Generally, this correction is small; however, when $E_N = E_0$, it is of order $\Delta E_{\text{hfs}}/Z$ and represents the first-order Coulomb correction to the wave function $|A\rangle$:

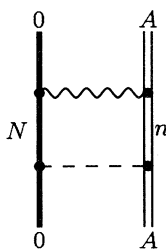


FIG. 2. Feynman graph describing the first-order Coulomb corrections to hfs. The dashed line corresponds to a Coulomb photon. The symbols N and n denote sums over the Dirac spectrum for the proton and electron, respectively.

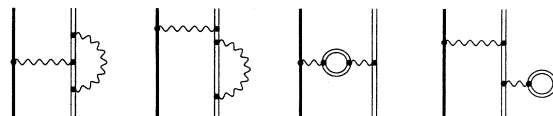


FIG. 3. Feynman graphs corresponding to the radiative corrections to hfs in the dynamic proton model.

$$\Delta E_{\text{hfs}}^{(1)} = \sum_{Nn} \frac{\langle 0A | V_{\text{Br}} | 0n \rangle \langle 0n | V_{\text{C}} | 0A \rangle}{\epsilon_A - \epsilon_n}. \quad (3)$$

The Feynman graph that differs from Fig. 2 by the interchange of photon lines gives the first-order Coulomb correction to the adjoint wave function $\langle A|$. The sum of the ladder graphs with many photon lines in all orders of perturbation theory leads to the replacement of the electron wave function for the potential $V^{(Z-1)}$ in Eq. (1) by the wave function for the electron in the corresponding potential $V^{(Z)}$. Below, we assume that this substitution has been made. We would like to mention that, in the dynamic proton model, radiative corrections to the hfs correspond to the Feynman graphs of Fig. 3. These graphs are similar to those for the screening of the Lamb shift considered recently for the He-like and Li-like ions [10–12]. It follows that the evaluation of radiative corrections in the dynamic proton model is straightforward and can be generalized naturally to higher orders.

III. ANGULAR INTEGRATION

To carry out the angular integrations in Eq. (1), we use the formula given in [13] for two-particle matrix element of the unretarded Breit operator. Since we use only diagonal matrix elements, there is no distinction between the retarded and unretarded Breit interaction. With the notation

$$m_{ILM', jlm'; ILM, jlm} = \left\langle \frac{\boldsymbol{\alpha}_p \cdot \boldsymbol{\alpha}_e}{r_{12}} \right\rangle_{ILM', jlm'; ILM, jlm}, \quad (4)$$

where the angular momentum quantum numbers ILM and jlm refer to the proton and electron, respectively, the result in Ref. [13] can be written

$$m_{ILM', jlm'; ILM, jlm} = \sum_{\lambda=0}^{\infty} J_{\lambda}(ILM', jlm'; ILM, jlm) \times N_{\lambda}(K, \kappa). \quad (5)$$

Here we use the following notation:

$$J_{\lambda}(ILM', jlm'; ILM, jlm) = \sum_{\mu} (-1)^{I+j+\lambda-M'-m'-\mu} \times \begin{pmatrix} I & \lambda & I \\ -M' & \mu & M \end{pmatrix} \times \begin{pmatrix} j & \lambda & j \\ -m' & -\mu & m \end{pmatrix}, \quad (6)$$

$$N_\lambda(K, \kappa) = (-1)^\lambda \frac{4K\kappa}{\lambda(\lambda+1)} \times C_\lambda(-K, K) C_\lambda(-\kappa, \kappa) Q_\lambda(K, \kappa), \quad (7)$$

and

$$Q_\lambda(K, \kappa) = \int_0^\infty dx \int_0^\infty dx' \frac{x^\lambda}{x^{\lambda+1}} [2g_K(x)f_K(x)] \times [2g_\kappa(x')f_\kappa(x')]. \quad (8)$$

In the above formulas, we use $K = \mp(I \pm 1/2)$ for $I = L \pm 1/2$ and $\kappa = \mp(j \pm 1/2)$ for $j = l \pm 1/2$. The quantities $C_\lambda(\kappa', \kappa)$ are given by

$$C_\lambda(\kappa', \kappa) = (-1)^{j'+1/2} \sqrt{(2j'+1)(2j+1)} \times \begin{pmatrix} j & \lambda & j' \\ 1/2 & 0 & -1/2 \end{pmatrix} \Pi(l, l', \lambda), \quad (9)$$

with

$$\Pi(l, l', \lambda) = \begin{cases} 1 & \text{if } l + l' + \lambda \text{ even} \\ 0 & \text{if } l + l' + \lambda \text{ odd} \end{cases}. \quad (10)$$

The functions $g_K(r)$ and $f_K(r)$ are the large and small components of the proton wave function, respectively; whereas, $g_\kappa(r)$ and $f_\kappa(r)$ are the large and small components of the electron wave function. It is important to note that the selection rules in Eq. (10) imply that $C_\lambda(-\kappa, \kappa) = 0$ unless λ is odd, so the sum in Eq. (5) extends over odd integers only. Coupling the wave functions for the electron and proton in Eq. (4) to angular momentum FM_F , leads to the expression

$$\Delta E_{\text{hfs}} = \sum_{M'm'} \sum_{Mm} \langle IM', jm' | FM_F \rangle \langle IM, jm | FM_F \rangle \times m_{ILM', jlm'; ILM, jlm}. \quad (11)$$

Summation over $M'm', Mm$ leads to

$$\Delta E_{\text{hfs}} = \sum_{\lambda=1}^{\infty} (-1)^{I+j+F+\lambda} \left\{ \begin{matrix} I & j & F \\ j & I & \lambda \end{matrix} \right\} N_\lambda(K, \kappa). \quad (12)$$

The selection rules in the $6j$ -symbol imply that $0 \leq \lambda \leq \min(2I, 2j)$. Formula (12) contains the interaction with all higher magnetic moments of the nucleus; the usual magnetic hyperfine interaction corresponds to $\lambda = 1$. Since the electronic ground state of $^{209}\text{Bi}^{82+}$ has $j = 1/2$, the only contribution is from the term with $\lambda = 1$. For this case, Eq.(12) reduces to

$$\Delta E_{\text{hfs}} = \frac{1}{2} [F(F+1) - I(I+1) - j(j+1)] a, \quad (13)$$

where the hyperfine constant a is given by

$$a = \frac{\kappa K}{2j(j+1)I(I+1)} Q_1(K, \kappa). \quad (14)$$

For $j = 1/2$, the separation between the states with $F = I + 1/2$ and $F = I - 1/2$ is just $(I + 1/2)a$. Equation (14) is used below to evaluate the hfs of $^{209}\text{Bi}^{82+}$.

IV. EXTERNAL FIELD LIMIT

It is of interest to examine the limiting case of Eq. (14) when the size of the proton orbit is vanishingly small with respect to the radius of the electronic orbit. In this case, the integral $Q_1(K, \kappa)$ separates into a product of two integrals

$$Q_1(K, \kappa) \rightarrow \int_0^\infty dx x [2g_K(x)f_K(x)] \times \int_0^\infty dx \frac{1}{x^2} [2g_\kappa(x)f_\kappa(x)]. \quad (15)$$

Using the fact that the nuclear gyromagnetic ratio of the proton, treated as a Dirac particle with no anomalous moment, is given by

$$g_I = -Mc \frac{K}{I(I+1)} \int_0^\infty dx x [2g_K(x)f_K(x)], \quad (16)$$

where M is the proton mass; we obtain for a the limiting expression

$$a \rightarrow a_{\text{static}} = -\frac{1}{2Mc} g_I \frac{\kappa}{j(j+1)} \int_0^\infty dx \frac{1}{x^2} [2g_\kappa(x)f_\kappa(x)]. \quad (17)$$

Equation (17) is the standard expression (in atomic units) relating the hyperfine constant a to the nuclear gyromagnetic ratio in the external field approximation [3].

Let us examine the expression (16) for g_I using the Pauli approximation,

$$f_K(r) \approx -\frac{1}{2Mc} \left(\frac{d}{dr} + \frac{K}{r} \right) g_K(r),$$

for the proton wave function. In this approximation, we obtain

$$g_I \approx \frac{K}{I(I+1)} \int_0^\infty dx x g_K(x) \left(\frac{d}{dx} + \frac{K}{x} \right) g_K(x) = \frac{K(K-1/2)}{I(I+1)}. \quad (18)$$

Here we assumed that, in the Pauli approximation, the large component of the proton wave function is itself normalized. The expression (18) is identical to the nonrelativistic Schmidt formula [14] for the g factor

$$g_I = \begin{cases} \frac{2L+2}{2L+1} g_L - \frac{1}{2L+1} g_s & \text{for } K > 0, \\ \frac{2L}{2L+1} g_L + \frac{1}{2L+1} g_s & \text{for } K < 0, \end{cases} \quad (19)$$

$$(20)$$

with $g_L = 1$ and $g_s = 2$. Thus, the present model reduces to the external-field approximation for the hyperfine constant a with a relativistic single-particle nuclear moment in the limit that the finite size of the proton orbit is ignored.

V. BOHR-WEISSKOPF EFFECT

In Ref. [3], the effects of a finite distribution of nuclear magnetism is examined within the framework of the Bohr-Weisskopf model using a probability distribution function for the odd proton deduced from a nuclear mean-field calculation. Here, the effects of a finite distribution of magnetism are included automatically in the basic equation (14). Let us write $Q_1(K, \kappa)$ in the form

$$Q_1(K, \kappa) = \int_0^\infty dx \frac{1}{x^2} [2g_\kappa(x)f_\kappa(x)] I(x), \quad (21)$$

with

$$I(x) = \int_0^x dx' x' [2g_K(x')f_K(x')] + x^3 \int_x^\infty dx' \frac{1}{x'^2} [2g_K(x')f_K(x')]. \quad (22)$$

We use the Pauli approximation to reduce the expression in braces to

$$I(x) \approx -\frac{K-1/2}{Mc} \int_0^x dx' g_K^2(x') - \frac{K+1}{Mc} \int_x^\infty dx' \frac{x^3}{x'^3} g_K^2(x'). \quad (23)$$

With the aid of this result, we may rewrite Eq. (21) in the form

$$Q_1(K, \kappa) \approx -\frac{K-1/2}{Mc} \int_0^\infty dx g_K^2(x) \times \int_0^\infty dx \frac{1}{x^2} [2g_\kappa(x)f_\kappa(x)] [1 - \epsilon(x)], \quad (24)$$

where

$$N_K^2 \epsilon(x) = \int_x^\infty dx' g_K^2(x') - \frac{K+1}{K-1/2} \int_x^\infty dx' \frac{x^3}{x'^3} g_K^2(x'), \quad (25)$$

with

$$N_K^2 = \int_0^\infty dx g_K^2(x).$$

The correction for the finite distribution of magnetization found in the Pauli approximation can be evaluated, therefore, by introducing the factor $\epsilon(x)$ into the integrand of the external-field equation (17):

$$a = -\frac{1}{2Mc} g_I \frac{\kappa}{j(j+1)} \int_0^\infty dx \frac{1}{x^2} [2g_\kappa(x)f_\kappa(x)] [1 - \epsilon(x)]. \quad (26)$$

This leads to a modification of Eq. (17), $a_{\text{static}} \rightarrow a_{\text{static}} - \delta a_{\text{BW}}$, where the correction to the hyperfine constant δa_{BW} is given by

$$\delta a_{\text{BW}} = \frac{1}{2Mc} g_I \frac{\kappa}{j(j+1)} \int_0^\infty dx \epsilon(x) \frac{1}{x^2} [2g_\kappa(x)f_\kappa(x)]. \quad (27)$$

The treatment of the Bohr-Weisskopf correction in Refs. [8,9] using $g_s = 2$ and $g_L = 1$ leads to precisely this expression. In summary, in the nonrelativistic limit, the dynamic proton model predicts a value of g_I corresponding to the Schmidt limit and includes the Bohr-Weisskopf corrections with a magnetization distribution function $g_K^2(r)/N_K^2$.

VI. NUMERICAL CALCULATIONS

As a first step in calculating the hfs of $^{209}\text{Bi}^{82+}$, we solve the radial Dirac equation for the proton, which is assumed to be moving in a Woods-Saxon central potential,

$$U(r) = -\frac{V_0}{\exp[(r-c)/a] + 1}, \quad (28)$$

with $c = c_0 A^{1/3}$ fm and $a = 0.5$ fm [14]. The depth of the potential well V_0 and c_0 are allowed to vary. The valence proton in ^{209}Bi has angular quantum number $K = 5$, corresponding to an $h_{9/2}$ state. In Table I, we give values of the eigenvalue E_p of the Dirac equation, which in the independent-particle approximation is the proton binding energy, for various values of V_0 and c_0 . Also shown in Table I are the root-mean-square radii of the proton orbits, R_{rms} . We adjust the parameters V_0 and c_0 to give the measured binding energy $E_p = -3.7977$ MeV [15] and to give $R_{\text{rms}} = 6.1769$ fm. This latter value is the root-mean-square radius of the magnetization distribution from a nuclear mean-field calculation obtained in [3]. We also give, in Table I, the relativistic gyromagnetic ratio g_I^{rel} obtained by evaluating Eq. (15) using the calculated proton wave function. The relativistic g factor is seen to be smaller than the nonrelativistic independent-particle limit $g = 10/11 = 0.909091$ (Schmidt) by about 3% throughout the parameter range considered. The adjusted values of the parameters in the Woods-Saxon potential are $V_0 = 33.879677$ MeV and $c_0 = 1.206470$ fm. The relativistic gyromagnetic ratio is $g_I^{\text{rel}} = 0.885221$, a factor of 1.031908 smaller than the experimental value $g_I^{\text{exp}} = 0.91347$ [16].

In the lower panel of Fig. 4, we plot the resulting Woods-Saxon potential $U(r)$ and the effective potential obtained by including the centrifugal barrier. In the up-

TABLE I. Proton binding energy E_p (MeV), root-mean-square radius R_{rms} (fm), and relativistic proton gyromagnetic ratio g_I^{rel} obtained by solving the Dirac equation in a Woods-Saxon potential with central radius $c = c_0 A^{1/3}$ (fm), thickness $a = 0.5$ (fm), and depth V_0 (MeV).

V_0	c_0	E_p	R_{rms}	g_I^{rel}
29	1.30	-3.2713	6.65	0.8883
30	1.30	-4.0710	6.60	0.8881
31	1.25	-3.1695	6.42	0.8869
32	1.25	-3.9605	6.37	0.8866
34	1.20	-3.6333	6.15	0.8850
35	1.20	-4.4214	6.12	0.8848

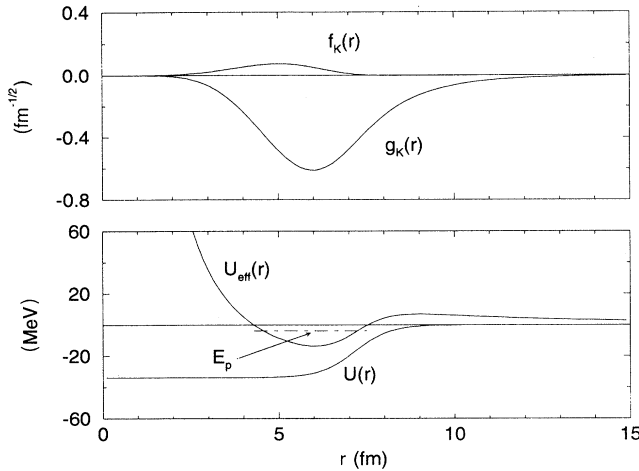


FIG. 4. Lower panel: nuclear Woods-Saxon potential with $V_0 = 33.879677$ MeV, $c = 1.206470A^{1/3}$ fm, and $a = 0.5$ fm is plotted together with the corresponding effective potential for a state with $L = 5$. The $1h_{9/2}$ eigenvalue is designated by E_p . Upper panel: large and small component radial Dirac wave functions for the $1h_{9/2}$ proton.

per panel of this figure, we plot the corresponding large and small components of the proton Dirac wave function obtained by solving the Dirac equation in this potential.

The electron Dirac wave function is evaluated in the field of a finite charge distribution defined by the charge density function,

$$\rho(r) = \frac{\rho_0}{\exp[(r - c_1)/a_1] + 1} \quad (29)$$

with $c_1 = 6.75$ fm and $a_1 = 0.468$ fm [17]. These parameters are identical to those used in Ref. [3]. The eigenenergy for the $1s_{1/2}$ electron in this potential is found to be $E_{1s} = -3833.6378$ a.u. With the wave function obtained in this potential, we evaluate the hyperfine structure exactly, using Eq. (14), and in the static limit, using Eq. (17). In both cases, we scale our results by the ratio of the observed magnetic moment to the calculated moment. Thus, in the static limit, our value of the hyperfine interval reduces to the corresponding value obtained in [3].

$$\Delta E_{\text{hfs}} = 238.814 \text{ nm} \quad (\text{static limit}),$$

and is independent of the proton potential. The values obtained in the dynamic model, of course, depend on the nuclear potential. For the potential chosen here, we find

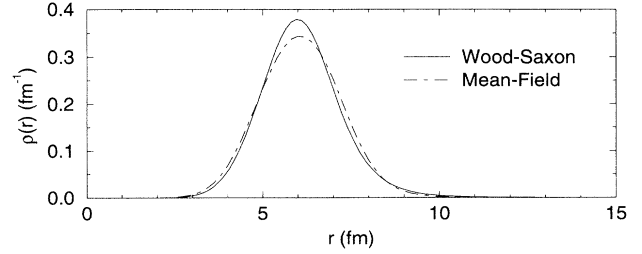


FIG. 5. Comparison of the magnetization distribution function $w(r)$ from a nuclear mean field calculation [3] and that from the present dynamic proton model.

$$\Delta E_{\text{hfs}} = 241.977 \text{ nm},$$

corresponding to a Bohr-Weisskopf shift of 3.163 nm.

It is of interest to compare the magnetization distribution function $w(r)$ used in [3] with that used in the present study, $g_K^2(r)/N_K^2$. For this purpose, we plot the two distribution functions in Fig. 5. Using the distribution $w(r)$, a value of 3.45 nm was found for the BW correction [3]. If we replace the present magnetic distribution function $g_K^2(r)/N_K^2$ by $w(r)$ in Eq. (25), we obtain a value of 3.11 nm for the correction. Thus, the BW correction is sensitive to both the radial shape of the radial distribution function and to assumptions concerning the angular symmetry of the spin.

The value from the dynamic model may be compared with the experimental value reported in [1]

$$\Delta E_{\text{expt}} = 243.87(4) \text{ nm},$$

to infer that the residual corrections are about 2 nm. These corrections consist of nuclear many-body corrections of the type considered in [6] and the QED corrections given in Fig. 3. The calculations of Ref. [6] indicate that the nuclear many-body corrections alone will give a value of the energy separation 243.54 nm, within 0.33 nm of the experimental value, indicating that the net QED correction is very small. Work is now in progress evaluating QED and nuclear corrections starting from the dynamic proton model.

ACKNOWLEDGMENTS

The work of W.R.J. was supported by the Alexander von Humboldt Foundation and the work of L.N.L. was supported by the Deutsche Forschungsgesellschaft (DFG). G.S. acknowledges support by GSI (Darmstadt), by BMFT, and by DFG.

- [1] I. Klaft, S. Borneis, T. Engel, B. Fricke, R. Grieser, G. Huber, T. Kühl, D. Marx, R. Neumann, S. Schröder, P. Seelig, and L. Völker, Phys. Rev. Lett. **73**, 2425 (1994).
- [2] M. Finkbeiner, B. Fricke, and T. Kühl, Phys. Lett. A **176**, 133 (1993).
- [3] S.M. Schneider, J. Schaffner, W. Greiner, and G. Soff, J.

Phys. B **26**, L581 (1993).

- [4] S.M. Schneider, W. Greiner, and G. Soff, Phys. Rev. A **50**, 118 (1994).
- [5] S.M. Schneider, H. Persson, and G. Soff (unpublished).
- [6] M. Tomaselli, S.M. Schneider, E. Kankleit, and T. Kühl Phys. Rev. C (to be published).

- [7] A. Bohr and V.F. Weisskopf, *Phys. Rev.* **77**, 94 (1950).
- [8] A. Bohr, *Phys. Rev.* **81**, 331 (1951).
- [9] M. LeBellac, *Nucl. Phys.* **40**, 645 (1963).
- [10] S.A. Blundell, *Phys. Rev. A* **46**, 3162 (1992).
- [11] I. Lindgren, H. Persson, S. Salomonson, and Y. Ynnerman, *Phys. Rev. A* **47**, 1 (1993).
- [12] I. Lindgren, H. Persson, S. Salomonson, and P. Sunnergren, *Phys. Rev. A* **48**, 2772 (1993).
- [13] W.R. Johnson, S.A. Blundell, and J. Sapirstein, *Phys. Rev. A* **37**, 2764 (1988).
- [14] J. Eisenberg and W. Greiner, *Nuclear Theory: Nuclear Models* (North-Holland, Amsterdam, 1970).
- [15] G. Audi and A.H. Wapstra, *Nucl. Phys. A* **565**, 1 (1993).
- [16] Y. Ting and D. Williams, *Phys. Rev.* **89**, 595 (1953).
- [17] H. de Vries, C.W. de Jager, and C. de Vries, *At. Data Nucl. Data Tables* **36**, 495 (1987).